

# Convective Instabilities of Bunched Beams with Space Charge

A. Burov\*

Fermilab, PO Box 500, Batavia, IL 60510-5011

(Dated: May 2, 2022)

Although the transverse mode coupling instability (TMCI) threshold normally increases linearly with the space charge tune shift, it is hard to benefit from that significantly: while the space charge (SC) suppresses TMCI, it introduces *saturating convective* and *absolute-convective* instabilities, SCI and ACI, which could make the beam even less stable than without SC. Due to this a convective instability should develop near the transition energy of hadron machines, while TMCI should be suppressed there. In particular, either SCI or ACI may be an explanation of SC-independence of the transverse instability at CERN SPS under its old Q26 optics, so far unexplained.

## I. ABSOLUTE AND CONVECTIVE INSTABILITIES

Transverse mode coupling instabilities (TMCI) are believed to be one of the main limitations for the intensity of bunched beams. Such single-bunch instabilities develop when the head-tail phase is small,  $\xi\sigma_\delta/Q_s \ll 1$ , where  $\xi$  is the chromaticity,  $\sigma_\delta$  is the relative rms momentum spread and  $Q_s$  is the synchrotron tune, so that the chromatic effects can be neglected, see e.g. Ref. [1]. For proton beams, an important question is: how does TMCI depend on the space charge (SC) tune shift  $\Delta Q_{sc}$ ? Since the latter is typically high for low and medium energy machines, where the SC parameter  $q = \Delta Q_{sc}/Q_s \gg 1$  even far from the transition energy, the question is really important.

According to Ref. [2–5], TMCI intensity threshold increases, with rare exceptions, proportionally to the SC tune shift; SC makes the bunch more stable in this respect. We called this dominating class of the mode-coupling instabilities *vanishing*, meaning that they vanish at sufficiently high SC, when the SC tune shift significantly exceeds the wake-related coherent tune shifts. For coasting beams, however, dependence of the transverse instability on SC is opposite: the threshold wake amplitude drops down as SC increases, since the latter suppresses Landau damping. This oppositeness may be especially puzzling in light of the similarity, if not identity, of the bunched and coasting beam thresholds without SC, clearly seen when the former is expressed in terms of the maximal line density and rms momentum spread, and the latter is supposed to be Gaussian or alike. This similarity was presumed long ago by approximate fast microwave transverse stability criterion for bunched beams [6]. The main idea behind it (as well as behind similar Keil-Schnell-Boussard criterion for the longitudinal direction) was one of a fast microwave instability, which occurs locally, so that neither synchrotron motion nor bunch density variation should be very important. Following this idea, it can be expected that the microwave criterion is rather accurate for short wakes,

and may be a reasonable estimation with correct scaling for arbitrary wakes. Indeed, the agreement of this criterion with the computed TMCI thresholds was found to be especially good for short wakes, i.e. long bunches; for details see Ref. [7]. Due to this similarity of the coasting beam stability criteria to the bunched one without SC, the theoretical statement of oppositeness of their dependence on SC raises a suspicion that something is lost in the picture. The suspicion is strengthened by measurements and tracking simulations at CERN SPS [8–11], especially for the old Q26 optics, showing, at best, only weak dependence of the instability thresholds on SC, or no dependence at all.

For both, coasting and bunched beams, the microwave instability can be considered in terms of time evolution of an initial wave packet, traveling opposite to the beam motion, due to the wake causality. If the wave packet grows, as it travels that way along the coasting beam, the beam is unstable. However, this may not be so for the bunched beam, where a similarly growing microwave packet may travel in that manner only for a finite length, up to the bunch tail, and for a finite time, shorter than a half of the synchrotron period; thus, its growth does not necessarily entail the collective instability. The same mechanism of interaction may cause instability in the coasting beam and only head-to-tail signal amplification in the bunch, without making the entire bunch unstable. To articulate this distinction, we may, following Landau and Lifshitz [12], use the terms *absolute* and *convective* to qualify instabilities: for the former, the initial perturbation causes an unrestricted exponential growth everywhere in the medium, while for the latter, there is only a spacial amplification, and the perturbation eventually decays everywhere when a dissipation is added, no matter how tiny. Thus, the absolute instability in the coasting beam may correspond to only a finite amplification along the similar bunch, i.e. to a convective instability, without the absolute growth of the initial perturbation. It is worth noting that even without SC the TMCI threshold may be much higher than the instability threshold of the corresponding coasting beam: for instance, this is the situation with the air-bag bunch in a square well, the ABS [13]. Due to the absence of Landau damping, the corresponding two-stream coasting beam instability is threshold-less, while the TMCI threshold for the ABS

\* burov@fnal.gov

model is finite. Apparently, without SC, the wave packet growth cannot be fast in comparison to the synchrotron motion in the bunch below TMCI; at least the author of this paper does not know any examples of that sort.

With SC, the situation changes, since for the dominant *vanishing* case, the TMCI threshold tends to grow proportionally to the SC tune shift, while the condition for the wave packet *to grow fast* benefits from SC due to its tendency to make the bunch slices rigid (see Ref [2] and multiple plots below). Thus, there should be an interval of wake amplitudes between the convective and absolute instability, and the width of this interval has to be proportional to the SC parameter. Note that contrary to the beam breakup in linacs, the discussed regime of the signal amplification does not lead to an infinite growth of the perturbation at the bunch tail; the amplification saturates due to the synchrotron oscillations. Indeed, with all the collective modes being stable, it is impossible to get an unlimited signal. However, on time intervals short compared to the synchrotron period, the amplification should grow similarly to the conventional beam breakup in linacs. To keep this further distinction, I call the convective instabilities below TMCI threshold *saturating convective instabilities*, SCI, while the beam breakup represents its alternative, an *unbounded convective instability*, UCI.

One more important feature of the convective instabilities is that they make the bunch much more prone to the absolute instability: even a weak tail-to-head action by means of a multibunch or over-revolution wake, negligible by itself, may be sufficient to make bunch oscillations unstable absolutely. Moreover, it is shown below that a damper of any sort, including the conventional bunch-by-bunch resistive kind, works as a generator of the absolute instability if the convective instability is present; thus, the convective instability turns the bunch into a sort of fragile metastable state. The absolute instability of such a combined kind may be called an *absolute-convective instability*, or ACI.

Below, the main features of convective transverse instabilities of bunched beams with SC are shown by means of the ABS model.

## II. ABS MODEL

### A. Description

The ABS model allows effective solutions of Vlasov equations for bunch transverse oscillations with arbitrary wake functions and SC tune shifts. For this model, it is convenient to measure coordinates  $s$  along the bunch as fractions of its full length, so that  $0 \leq s \leq 1$ , and to measure time  $\theta$  in synchrotron radians, so the synchrotron period  $T_s = 2\pi$ . The wake functions can be dimensionless by measuring them in units of their amplitudes, specified for each case. After that, equations of motion of the positive and negative fluxes of the ABS bunch in

terms of their complex amplitudes  $x^\pm(\theta, s)$  can be presented as follows

$$\begin{aligned} \frac{\partial x^+}{\partial \theta} - \frac{1}{\pi} \frac{\partial x^+}{\partial s} &= \frac{iq}{2}(x^+ - x^-) + iF, \\ \frac{\partial x^-}{\partial \theta} + \frac{1}{\pi} \frac{\partial x^-}{\partial s} &= \frac{iq}{2}(x^- - x^+) + iF, \\ F(\theta, s) &= w \int_0^s ds' W(s-s') \bar{x}(\theta, s'), \end{aligned} \quad (1)$$

where the local centroid offset  $\bar{x} = (x^+ + x^-)/2$ , and the boundary conditions

$$x^+ = x^- \text{ at } s = 0, 1. \quad (2)$$

Here the SC parameter  $q$  is the ratio of the SC tune shift to the synchrotron tune, and  $w$  is the wake parameter:

$$w = \frac{N_p W_0 r_0 R_0}{4\pi \gamma \beta^2 Q_\beta Q_s}. \quad (3)$$

with  $N_p$  as the number of particles per bunch,  $W_0$  as the wake amplitude,  $r_0$  as the classical radius,  $R_0$  as the average radius of the machine,  $\gamma$  and  $\beta$  as the relativistic factors,  $Q_\beta$  and  $Q_s$  as the betatron and the synchrotron tunes.

It may be useful to note that by virtue of Eqs. (1, 2) the space derivatives of the two offset amplitudes,  $x^+$  and  $x^-$ , are opposite at the bunch edges,  $\partial x^+/\partial s = -\partial x^-/\partial s$  at  $s = 0, 1$ .

An alternative way to represent Eqs. (1, 2) opens if we consider the fluxes  $x^+$  and  $x^-$  as two parts of a single circulation  $x(\psi)$  in the longitudinal phase space, with the synchrotron phase  $\psi$  running from  $-\pi$  to 0 for  $x^+$  part, and continuing to run from 0 to  $\pi$  for  $x^-$ . In other words,

$$x(\psi) = \begin{cases} x^+(s), & \text{with } \psi = -\pi s, & -\pi \leq \psi \leq 0; \\ x^-(s), & \text{with } \psi = \pi s, & 0 \leq \psi \leq \pi. \end{cases} \quad (4)$$

This representation automatically takes into account the boundary condition (2) and turns two dynamic equations (1) into one on the circulating flux  $x(\theta, \psi)$ :

$$\frac{\partial x}{\partial \theta} + \frac{\partial x}{\partial \psi} = \frac{iq}{2}[x(\psi) - x(-\psi)] + iF, \quad (5)$$

with  $\bar{x} = [x(\psi) + x(-\psi)]/2$ . By virtue of the periodicity on the synchrotron phase  $\psi$ , the circulation  $x$  can be expanded into a Fourier series

$$x(\theta, \psi) = \sum_{n=-\infty}^{\infty} A_n(\theta) \exp(in\psi). \quad (6)$$

After that, the problem is reduced to a set of ordinary differential equations on the time-dependent Fourier coefficients  $A_n(\theta)$ :

$$i\dot{A}_n = n - \frac{q}{2}(A_n - A_{-n}) - w \sum_{m=-\infty}^{\infty} U_{nm} A_m, \quad (7)$$

$$U_{nm} \equiv \int_0^1 ds \int_0^s ds' W(s-s') \cos(\pi ns) \cos(\pi ms')$$

In this form, the equations of motion can be easily solved with a proper truncation of the Fourier sums; number of calculated matrix elements  $U_{nm}$  is reduced  $\sim 8$  times if one notes that  $U_{nm} = U_{|n||m|} = (-1)^{n-m} U_{mn}$ . For those wakes when the integral  $U_{nm}$  can be taken analytically, the problem can be solved at contemporary laptop with any reasonable accuracy for a negligible time.

### B. Eigensystem

Without accounting for wakes, the ABS eigensystem,  $x_k \propto \exp(-i\nu_k\theta)$ , has been described in the original Ref. [13]:

$$\begin{aligned} \nu_k &= -q/2 \pm \sqrt{q^2/4 + k^2}; \\ x_k^\pm(s) &= C_k(\cos(k\pi s) \mp i \sin(k\pi s) \omega_k/k); \end{aligned} \quad (8)$$

for  $k = 0$ ,  $\nu_0 = 0$ ,  $x_0^\pm = C_0$ , and  $\nu_k > 0$  at  $k > 0$ . Hereafter, the normalization constants  $C_k$  are chosen so that the ABS eigenfunctions are of the unit norm:

$$\int_{-\pi}^{\pi} \frac{d\psi}{2\pi} |x_k|^2 = \int_0^1 ds \frac{|x_k^+|^2 + |x_k^-|^2}{2} = \sum_{n=-\infty}^{\infty} |A_{nk}|^2 = 1. \quad (9)$$

At zero SC,  $\nu_k = k$ ; thus, in this simplest case the eigenfunctions  $x_k(\theta, \psi)$  are just plain traveling waves,  $x_k(\theta, \psi) = \exp(-ik(\theta - \psi))$ , yielding standing waves for the centroid oscillations,  $\bar{x}_k = \cos(\pi ks) \exp(-ik\theta)$ .

At high SC, i.e. at  $q \gg 2|k|$ , the low-order modes almost degenerate:  $\nu_{+k} \approx k^2/q$ ,  $\nu_{-k} \approx -q - k^2/q$ . This spectrum tells that at high SC, the two fluxes oscillate almost identically,  $x^+ \approx x^-$  for the positive modes, and they are in the opposite phases for the negative modes,  $x^+ \approx -x^-$ , which is indeed the case. The lowest no-wake and strong SC eigenfunctions are demonstrated in Fig. 1. Contrary to no-SC case, the eigenfunctions  $x_l$  are pretty much standing waves here; their phases  $\arg x_l$  do not run, but stay constant, close to  $\pi$  for the positive modes and  $\pi/2$  for the negative ones, jumping by  $\pi$  at the function nodes. These specific values of the phases show that the fluxes  $x^+$  and  $x^-$  are almost in phase for the positive modes and almost out of phase for the negative. This transfer from the traveling waves at zero SC to the standing waves at strong SC follows directly from the equation of motion (5) for the no-wake case,  $F = 0$ . For zero SC, the eigenfunctions of Eq. (5) are ones of the translation generator  $\partial/\partial\psi$ , which are complex exponents,  $\exp(i l \psi)$ . At strong SC, the equation's eigenfunctions have to be eigenfunctions of the dominating SC operator which core  $\propto \delta(\psi - \psi') - \delta(\psi + \psi')$ ; thus, they must have a certain parity with the phase  $\psi$ , being either even (positive modes and zero mode) or odd (negative modes). Since SC mixes every Fourier harmonic  $n$  only with its opposite,  $-n$ , these eigenfunctions can be only even and odd combinations of  $\exp(in\psi)$  and  $\exp(-in\psi)$ , i.e. they can be only  $\cos(n\psi)$ , for the positive modes, and  $\sin(n\psi)$ ,

for the negative ones. Figure 2 shows stroboscopic snapshots of the centroid oscillations for the same no-wake and strong SC case, as Fig. 1, i.e. overlapping plots  $\Re(\bar{x} \exp(-i\theta_s))$ , with the stroboscope time  $\theta_s = 2\pi j/N_s$ ,  $j = 0, 1, \dots, N_s - 1$ , and  $N_s$  as an adjustable integer number. Note that with the same pattern of the identically normalized opposite modes,  $l$  and  $-l$ , their centroid amplitudes differ at strong SC by a factor of  $|l|/q \ll 1$ .

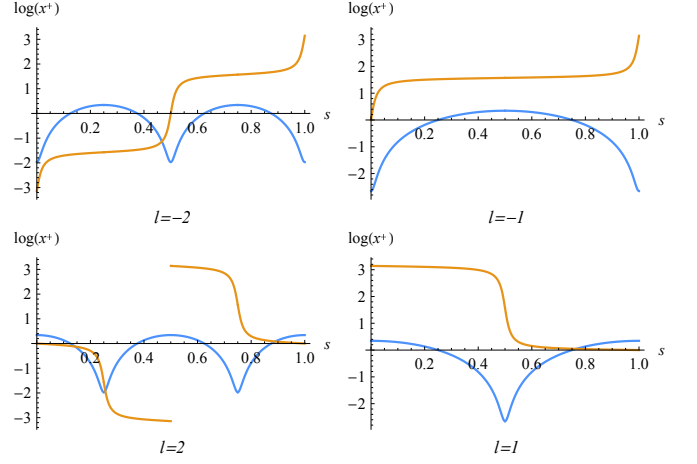


FIG. 1. No-wake ABS eigenfunctions for strong SC,  $q = 20$ , with their order  $l$  written below each plot. The blue line shows natural logarithms of the absolute values,  $\log |x_l^+(s)|$ ; the orange line represents the complex arguments  $\arg x_l^+(s)$ .

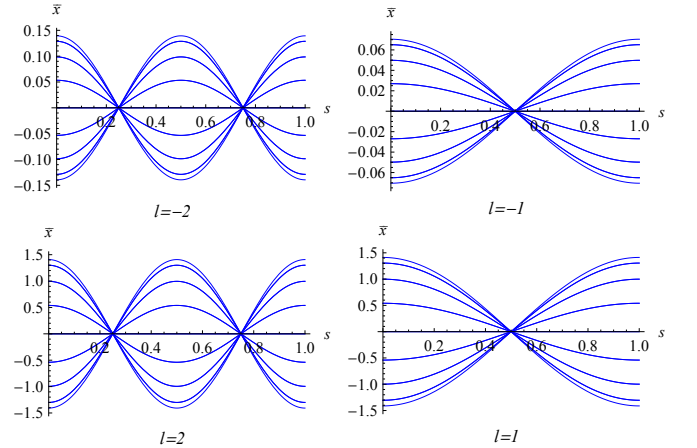


FIG. 2. Stroboscopic snapshots of the centroid oscillations for the same case,  $w = 0$ ,  $q = 20$  and modes,  $l = \pm 1, \pm 2$ , as Fig. 1 above. The opposite modes,  $l$  and  $-l$ , show the same pattern,  $\bar{x}_l(s) \propto \cos(\pi ls)$ , but the amplitudes differ by a large factor  $|l|/q$ , reflecting almost in phase oscillations of  $x^+$  and  $x^-$  for the positive modes and almost out of phase ones for the negative modes.

With wake on, the eigenfrequencies  $\nu_k$  shift from their no-wake values (8), and, if the wake is large enough, they couple, giving rise to the transverse mode coupling insta-

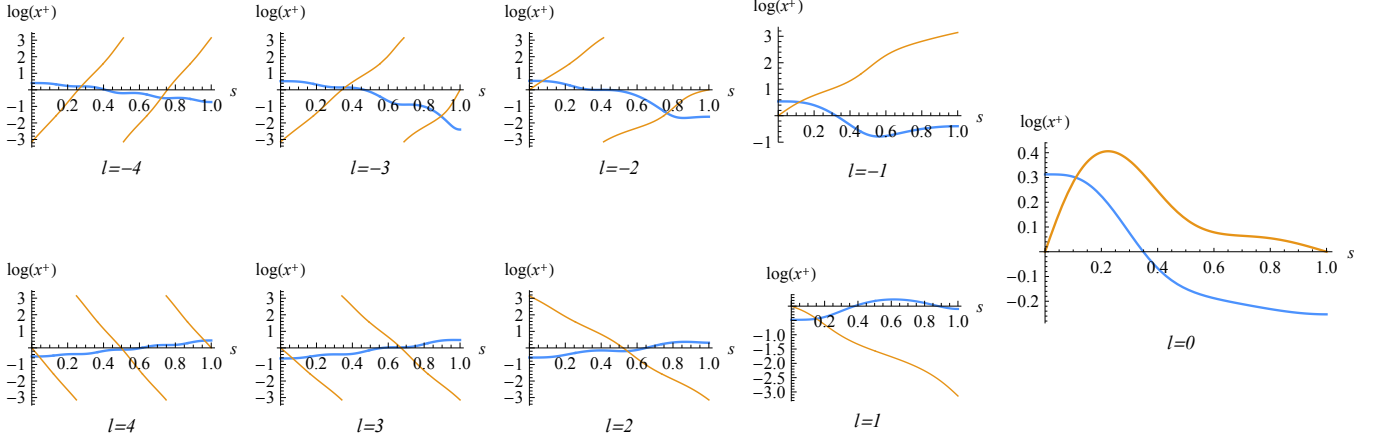


FIG. 3. Same as Fig. 1, but for no-SC and the wake parameter  $w = 13$ , which is slightly below the TMCI threshold,  $w_{\text{th}}^0 = 15$ , where the modes  $-2$  and  $-3$  couple. Note the general traveling wave pattern for all modes and that the pre-coupled negative modes are considerably head-dominated, contrary to the positive modes.

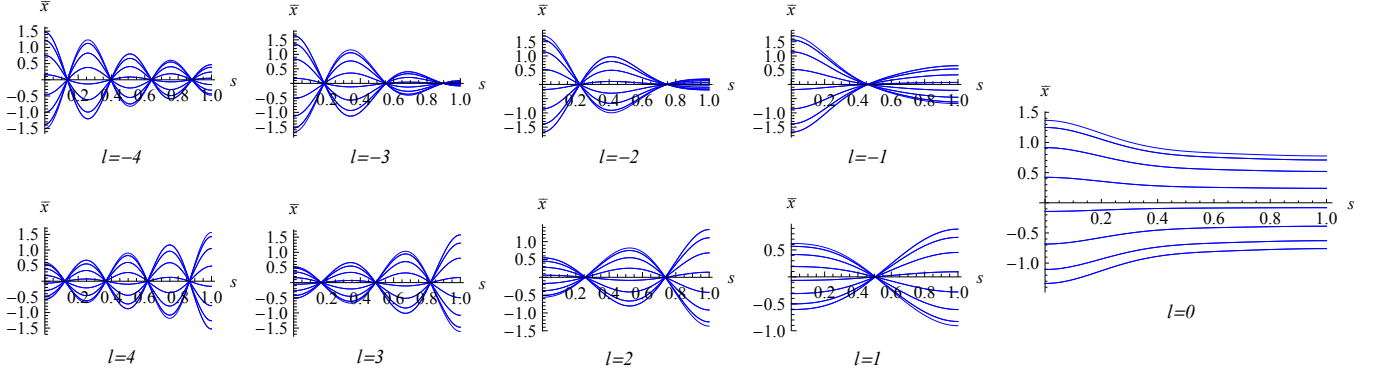


FIG. 4. Stroboscopic images of the centroid oscillations for the same parameters and modes as in Fig. 3. Each mode has as many nodes, as the modulus of its number.

bility, TMCI. Whatever the wake, some general features of the eigenfunctions can be stated.

- Without any loss of generality, the eigenfunctions  $x_k^+$  and  $x_k^-$  at the head of the bunch can be taken as the same real number:  $\Im(x_k^\pm(0)) = 0$ .
- Due to the symmetry of Eqs. (1) and their boundary conditions (2),  $x_k^-(s) = x_k^{+*}(s)$  for any eigenfunction  $k$  with real eigenfrequency  $\nu_k$ , where  $*$  means the complex conjugate. Hence, the amplitudes are real at the tail end,  $x_k^\pm(1) = x_k^\pm(1)$ .
- It follows, that for the modes with real frequencies  $\nu_k$  the head-to-tail phase advances  $\mu_k$  of  $x_k^\pm(s)$  are multiples of  $\pi$ ,  $\mu_k = \mp\pi k$ . The centroid  $\bar{x}_k(s)$  is a real function for such modes, which number of zeroes (nodes) is equal to the modulus of the mode number.

Following Ref. [2], we use a term *strong SC*, meaning that the SC tune shift considerably exceeds all other tune shifts. In other words, it means that the SC parameter  $q$  is large in comparison with the mostly involved

modes' numbers  $|l|$  and with the wake-driven coherent tune shifts  $\simeq wU_l$ , i.e.  $q \gg l$ , and  $q \gg w/w_{\text{th}}^0$ , where  $w_{\text{th}}^0 \simeq \min_l |U_l|^{-1}$  is TMCI threshold value of the wake parameter at zero SC. At strong SC, the wake cannot effectively mix positive and negative modes. Thus, for strong SC, the separation between positive modes, coupled with wake, and negative modes, uncoupled with it, is effective with wake as well as without it; hence, only positive modes may play a role, i.e. the bunch longitudinal slices are rigid [2].

Examples of the eigenfunctions, without and with SC, are presented in Figs. 3 - 6 for the broadband resonator wake

$$W(s) = \exp(-\alpha_r s) \sin(\bar{k} s), \quad (10)$$

with  $\alpha_r = k_r/(2Q_r)$ ,  $\bar{k} = \sqrt{k_r^2 - \alpha_r^2}$ ,  $Q_r = 1$ . To make an accent on long bunches, especially interesting for many proton machines, a rather short resonator wake was taken, which phase advance over the bunch length  $k_r = 10$ . The wake parameter  $w = 13$ ; it is chosen to be rather close to the no-SC TMCI threshold,  $w_{\text{th}} = 15$ .

Several features of these eigenfunctions deserve to be noted:

- For the no-SC case, the phases run pretty much linearly, similarly to the no-wake no-SC case.
- For the strong SC, the phases are mostly constant, quickly changing by  $\pm\pi$ . For the negative modes, the phases are mostly close to  $\pm\pi/2$ , which means that the two fluxes,  $x^+$  and  $x^-$ , oscillate in counter-phase. For the positive modes, the phases are mostly close to 0 or  $\pm\pi$ , showing that the two fluxes move together. These features are again similar to the no-wake case of Fig. 1.
- Without SC, the modes  $-2$  and  $-3$  couple at the wake parameter  $w_{\text{th}} = 15$ , just slightly above  $w = 13$  of Figs. 3 - 6. These pre-coupled modes are dominated by the head, being  $\sim q$  times larger there than at the tail.
- At the strong SC, negative modes are not sensitive to wake, while the positive modes steeply rise to the tail, showing something like cobra shapes, with the bunch tail as the cobra head, though. The reason is that at strong SC, the two bunch fluxes oscillate almost in opposite phases for negative modes, almost cancelling their wake forces. Contrary to that, for the positive modes, the fluxes oscillate together, their wake fields add, which results in the *convective instability*, well seen in Figs. 5, 6.

Having discussed the way the convective instabilities show themselves through the eigensystems, we may exercise another, complementary, way to look at them: the initial conditions, or Cauchy, problem.

### III. CAUCHY PROBLEM FOR ABS

#### A. Difference Scheme

Perhaps, the most straightforward method to solve at this point the Cauchy problem is one suggested by the Fourier form of Eq. (7). For the sake of diversity, though, as well as for a possibility of cross-checking, the author of this paper prefers to use another, not less effective, method of solution: a simple first-order numerical difference scheme, applied to the original equation of motion (1) with the boundary condition (2). The time derivative there can be taken as

$$\frac{\partial x}{\partial \theta} \approx (x_{\mu+1,p} - x_{\mu,p})/\Delta\theta.$$

for both  $+$  and  $-$  fluxes, where the Greek characters enumerate the time steps, and the Latin ones,  $p = 1, 2, \dots, P$ , are used for the space;  $\Delta\theta \ll 1$  and  $\Delta s = 1/(P-1) \ll 1$  are the time and space steps respectfully. To make the

algorithm numerically stable, the space derivatives have to be taken in accordance with the flux direction:

$$\frac{\partial x^+}{\partial s} \approx (x_{\mu,p+1}^+ - x_{\mu,p}^+)/\Delta s, \quad (11)$$

$$\frac{\partial x^-}{\partial s} \approx (x_{\mu,p}^- - x_{\mu,p-1}^-)/\Delta s, \quad (12)$$

and the Courant condition  $\Delta\theta < \pi\Delta s$  has to be satisfied. The boundary conditions, Eq. (2), allow to express  $x^\pm$  when the spacial indices step outside the bunch length:

$$x_{\mu,P+1}^+ = x_{\mu,P-1}^-, \quad x_{\mu,0}^- = x_{\mu,2}^+. \quad (13)$$

With these substitutions, as well as a first-order transformation of the wake integral into a sum, the resulting equations for a  $2P$ -component vector  $\mathbf{X}_\mu = (\mathbf{x}_\mu^+, \mathbf{x}_\mu^-)$ , composed of two  $P$ -component vectors  $\mathbf{x}_\mu^\pm$ , can be written in a matrix form

$$\mathbf{X}_{\mu+1} = \mathbf{X}_\mu + \Delta\theta \mathcal{L} \cdot \mathbf{X}_\mu, \quad (14)$$

where  $\mathcal{L}$  is the time-independent infinitesimal  $2P \times 2P$  generator matrix. From here, the sought-for vector at given time  $\theta$  can be represented as

$$\mathbf{X}(\theta) = \exp(\theta \mathcal{L}) \mathbf{X}(0) = (\mathcal{I} + \Delta\theta \mathcal{L})^{N_\theta} \mathbf{X}(0), \quad (15)$$

where  $N_\theta = \theta/\Delta\theta$  is a total number of the time steps,  $\mathcal{I}$  is  $2P \times 2P$  identity matrix, and  $\mathbf{X}(0)$  is a  $2P$ -vector of the initial conditions. The described numerical method reduces the problem to raising a  $2P \times 2P$  matrix to a power  $N_\theta \gg 1$ . Note that this computation can be performed with only  $\log_2(N_\theta)$  matrix multiplications, if the number of time steps  $N_\theta$  is made an integer power of 2, making the numerical scheme extremely efficient.

#### B. TMCI and Convective Instability

Let us start from the simplest example of the Heaviside step wake  $W(s) = \Theta(s)$ , where some analytical estimations are possible and not cumbersome, and which presents an alternative to the short broadband wake considered in the previous section. For short time intervals  $\theta \ll 1$ , the synchrotron motion can be neglected. Assuming the head-tail amplification coefficient  $K$  to be large enough, its natural logarithm can be estimated:

$$\log K \simeq 2(iw\theta)^{1/2}. \quad (16)$$

Hence, the maximally achievable amplification scales as

$$\log K \propto \sqrt{w}. \quad (17)$$

This statement can be checked by means of the described solution of the Cauchy problem for the ABS model. Without SC, its TMCI threshold is  $w_{\text{th}} = 1$ , see Refs. [5, 13].

Figures 8, 9 show the results of evolution after 1.5 synchrotron periods of the constant initial offset  $x_\pm(s) = 1$ ;

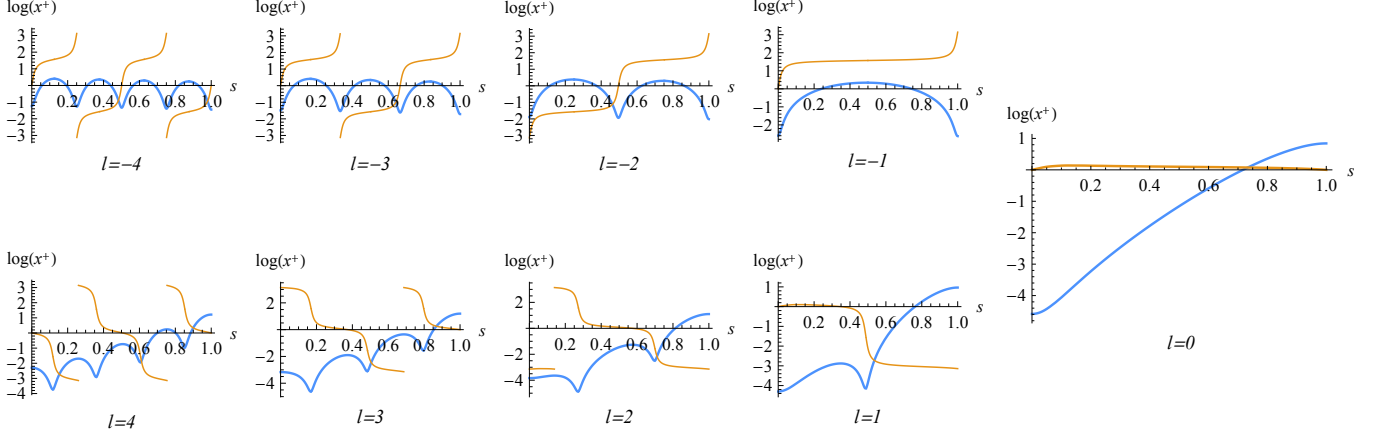


FIG. 5. Eigenfunctions with the broadband resonator wake, Eq. (10), wake and SC parameters  $w = 13$ ,  $q = 20$ ; compare with Figs. 1, 3. At that strong SC, the wake parameter  $w$  is  $\simeq 9$  times below the TMCI threshold. Blue lines show natural logarithms of the amplitudes  $\log |x_l^+|$ ; the orange ones are reserved for the phases  $\arg(x_l^+)$ . All the modes are absolutely stable,  $\Im \nu_l = 0$ , while head-to-tail amplification for the non-negative modes may exceed 100 for these parameters; note the *cobra shapes*, typical for these convective instabilities. Contrary to that, the negative modes look identical to their no-wake shapes of Fig. 1: with the out of phase motion of the  $+$  and  $-$  fluxes, the wake fields of the fluxes almost cancel each other.

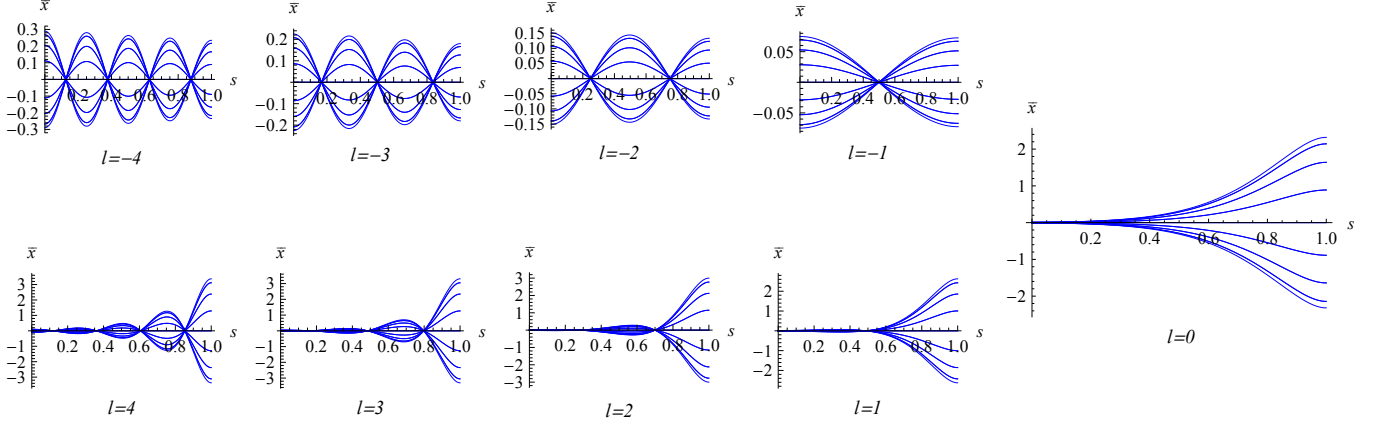


FIG. 6. Stroboscopic images of the centroid oscillations for the same parameters and modes as in Fig. 5. Number of nodes for each mode is identical to the modulus of its number.

the wake parameters are  $w = 1$  and  $w = 20$  correspondingly, and the SC parameter  $q = 20$ . It has been separately checked that the amplification reaches its limit after  $\sim 1$  synchrotron period, so for both cases the bunch is stable in the absolute sense, notwithstanding its wake being 20 times above the no-SC threshold for the latter case. Several things are worth mentioning for these plots:

- At the no-SC threshold,  $w = 1$ , the convective amplification is already significant,  $K \simeq 10$ .
- The two fluxes expectably oscillate in phase: out of phase oscillations are detuned by the SC tune shift from the wake-coupled motion of the centroid  $(x^+ + x^-)/2$ . That is why SC boosts head-to-tail signal amplification, making the bunch longitudinal slices rigid.
- The convective instability leads to the acclivitous

cobra shape of the amplitudes  $|x^\pm|$ , with zero derivative at the bunch tail.

- While the wakes differ by a factor of 20, the logarithms of the amplification confirm the scaling (17), showing that they differ by a factor close to  $\sqrt{20}$ .
- These plots make it possible to fit the numerical factor for the amplification (17) for the ABS model with the step-like wake:  $\log K \simeq 2\sqrt{w}$ .

After this brief examining of the theta-wake, let us come back to the broadband wake, Eq. 10, with the same phase advance  $k_r = 10$  and the quality factor  $Q_r = 1$  as above, to compare the complementary results of the eigensystem problem and the Cauchy problem with constant initial condition,  $x^\pm = 1$ , for that physically interesting case.

Figure 10 demonstrates evolution of the standard initial conditions  $x^\pm = 1$  after 8 synchrotron periods for

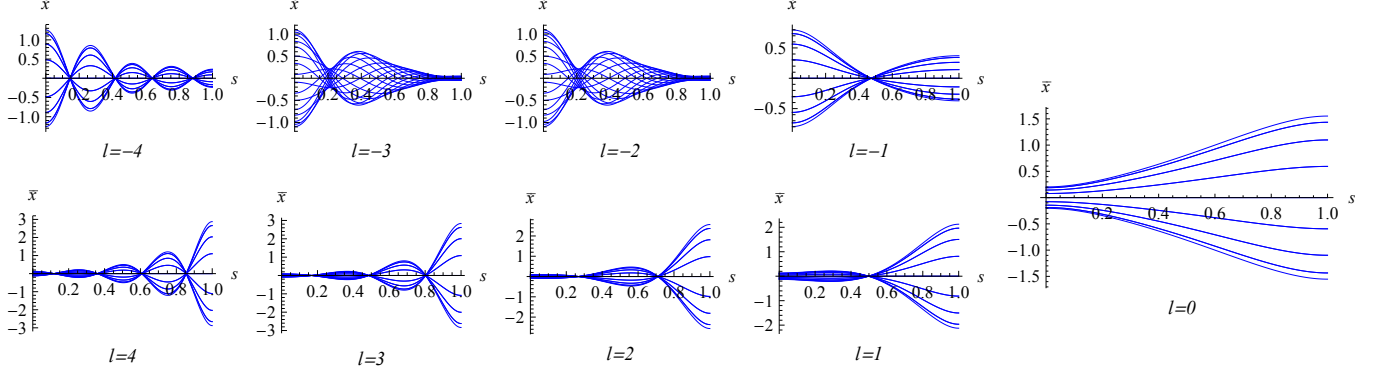


FIG. 7. Centroid oscillations for a moderate SC,  $q = 4.1$  and  $w = 35$ , which is a bit above the TMCI threshold  $w_{\text{th}} = 30$  at this SC parameter, twice as high as at zero SC. Nodes of the coupled modes  $l = -2$  and  $l = -3$  become waists. Note that head-dominated TMCI of the negative modes is complemented by tail-dominated SCI of the positive ones.

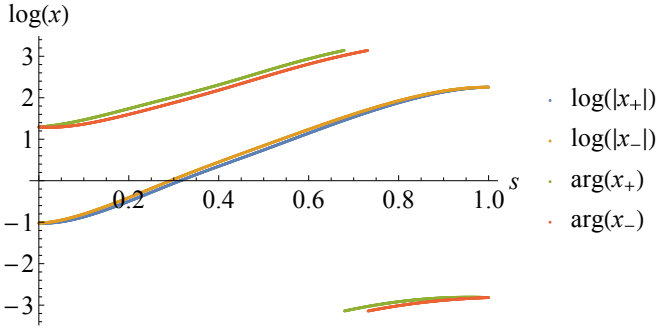


FIG. 8. Evolution of constant initial offset  $x^\pm(s) = 1$  after 1.5 synchrotron periods, with the SC parameter  $q = 20$ , step wake at the no-SC threshold,  $w = 1$ . Natural logarithms of the absolute values and complex arguments of the amplitudes  $x^\pm$  are shown. Note that the complex amplitudes of the fluxes are almost identical,  $x^+ \approx x^-$ .

the same wake and SC parameters as in Fig. 7,  $q = 4.1$  and  $w = 35$ , slightly above the TMCI threshold wake value  $w_{\text{th}} = 30$  at this SC, twice as it is at no SC case. Identity of this pattern with ones of the coupled eigen-

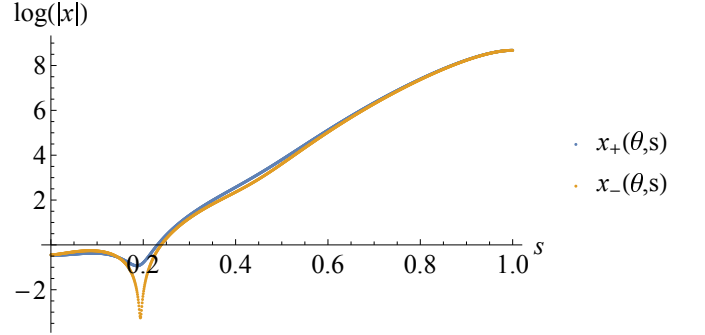


FIG. 9. Same as the previous figure, but with 20 times larger wake,  $w = 20$ . With that high amplification, the oscillations are still absolutely stable, as they must be, since the wake is below its threshold value. Note the cobra shape, typical of the SCI.

functions  $l = -2$  and  $l = -3$  of Fig. 7 serves as a good cross-check.

Figure 11 shows what happens at  $w = 13$  and  $q = 20$  with the initial perturbation,  $x^\pm = 1$ , after 1.5 synchrotron periods; the amplification coefficient can be



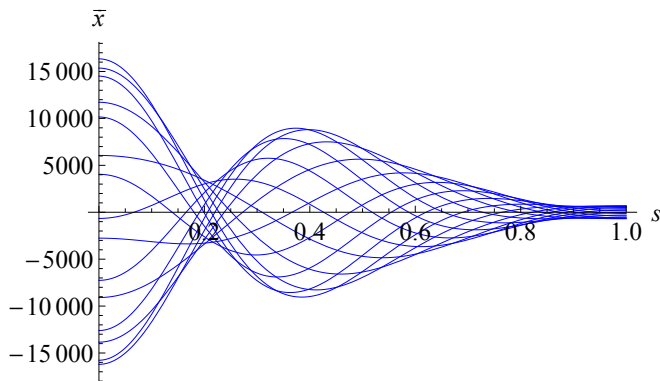


FIG. 10. Evolution of the standard initial conditions  $x^\pm = 1$  after 8 synchrotron periods for the same wake and SC parameters as in Fig. 7,  $q = 4.1$  and  $w = 35$ , slightly above the TMCI threshold wake value  $w_{th} = 30$  at this SC, twice as it is at no SC case. Identity of this pattern with the coupled eigenfunctions  $l = -2$  and  $l = -3$  of Fig. 7 serves as a good cross-check.

compared with such of zero mode of the related Fig 5. The convective instability saturation is demonstrated by the 3D plot of Fig 12. Contrary to the absolute instabilities, for the convective ones there is no selection with time of the most unstable mode, since all the modes are stable in the absolute sense, all the growth rates are zeroes. That is why the practically dominating constant initial perturbation excites several modes, and none of them is going to be stressed at the following evolution. As a results, the nodes of one convectively unstable mode overlap with antinodes of the neighbor modes, excited by the same initial perturbation, which smears all the nodes. Thus, no nodes have to be observed for the convective instability, unless a special mode is carefully excited at the beginning. This statement is illustrated by Fig. 13, showing the centroid stroboscopic plot after 1.5 synchrotron periods for  $q = 20$  and  $w = 13$ , i.e. for the same conditions as in Fig. 12.

Since strong SC makes the bunch slices rigid, and thus, maximally coupled with wake, with strong SC the bunch may get considerably more unstable than without it; this is demonstrated by Fig. 14 showing significant convective amplification at  $q = 20$  and  $w = 7$ , i.e. for the wake parameter of a half the no-wake TMCI threshold.

### C. Absolute-Convective Instability

The considerations and examples above demonstrate one important thing. Although at strong SC TMCI *vanishes*, it does not mean that in reality the beam becomes much more stable: the amplification of the saturating convective instability, SCI, can be intolerably large already at the wake parameter corresponding to the no-SC TMCI threshold, if not below that, so SCI may well be not any less dangerous than the TMCI. Moreover, the

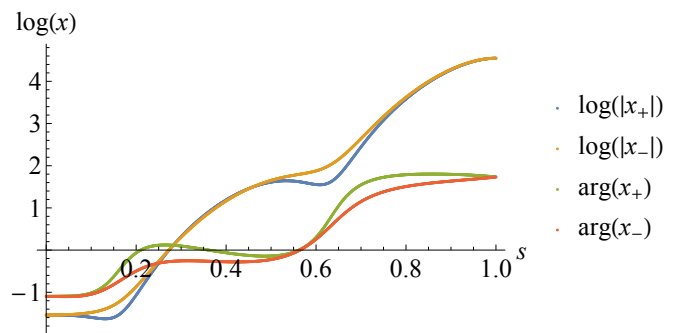


FIG. 11. Evolution of the standard initial perturbation after 1.5 synchrotron periods for the wake parameter  $w = 13$  and strong SC,  $q = 20$ . Note that the two amplitudes are close; compare with Fig. 5.

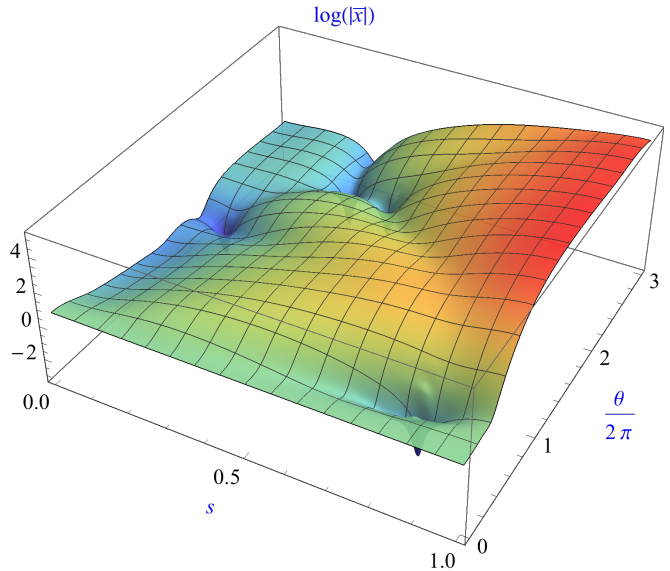


FIG. 12. Time evolution of the local centroids  $\bar{x}(\theta, s) = [x^+(\theta, s) + x^-(\theta, s)]/2$  for the same case, i.e. for  $q = 20$ ,  $w = 13$  and constant initial conditions,  $x^\pm = 1$ . The amplification is saturated within  $\sim 1$  synchrotron period.

SCI, dangerous by itself, opens a door for one more type of instability. With high convective amplification, even a weak tail-to-head feedback by means of a multibunch or over-revolution wake, negligible by itself, may be sufficient to make the beam unstable in the absolute sense. The convective instability may work as a huge amplification of the otherwise insignificant mechanism of an absolute instability. In this respect, the convective instability constitutes a sort of fragile metastable state. The absolute instability generated by such amplification may be called *absolute-convective instability*, or ACI.

The simplest way of modeling the tail-to-head over-revolution wake is to add to both right-hand-sides of Eqs. (1) a center-of-mass anti-damper term  $g \int_0^1 ds \bar{x}(s)$ , where  $g$  is the gain. Taken by itself, this term would drive an instability with the growth rate  $g$  per synchrotron ra-



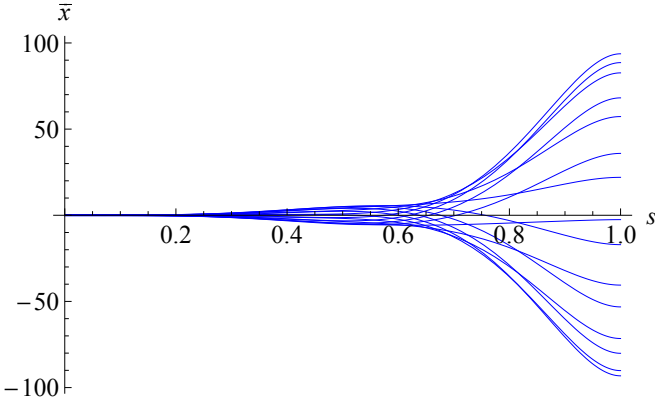


FIG. 13. Stroboscopic image of the beam centroid for the same parameters as in Fig. 12 after 1.5 synchrotron periods. Note that there are no nodes.

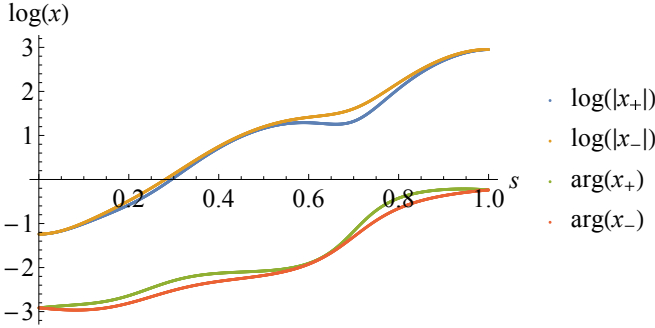


FIG. 14. Same as Fig. 11, but with weaker wake  $w = 7$ , i.e. 2 times lower than the no-SC TMCI threshold. Thus, with strong SC the bunch may get considerably more unstable than without it.

dian, or  $2\pi g$  per synchrotron period. With the convective instability, the absolute growth rate, caused by the same gain, can be significantly larger. An example of such a dramatic amplification of the growth rate is shown in Fig. 15. For this case, the growth rate is  $\sim 6$  times higher than the anti-damper gain would provide alone. Note that the ACI looks similar to SCI, having alike cobra shape and rigid slices.

At this point, one may ask the following. If convective instabilities amplify external anti-damping, turning it into a much faster ACI, wouldn't they enhance external damping as well, making its effect even more stabilizing? Well, the answer is worse than a simple no. In fact, the convective instability turns any damper, with whatever phase, into an ACI generator. This statement deserves to be doubly stressed, since it may seem counter-intuitive: yes, even a normal bunch-by-bunch resistive damper works as an ACI generator, even for moderately amplified convective instability, considerably below the no-SC threshold; Figs. 16 and 17 present an example. To be more precise, it may be said that the damper is just useless, if its gain is too small; then, with a higher gain, the damper shows itself as an enhancer of the

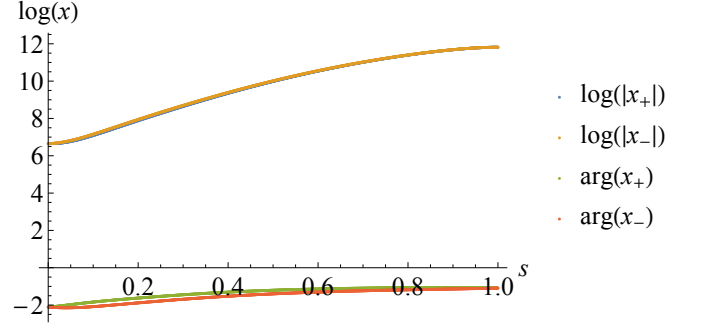


FIG. 15. Evolution of the constant initial conditions  $x^\pm(s) = 1$  after time  $\theta = 32 \cdot 2\pi$ , or 32 synchrotron periods, with the gain so small that  $g\theta = 1$ . The growth rate is  $\sim 6$  times higher than what the gain provides by itself. The wake phase advance  $k_r = 10$ , the SC parameter  $q = 20$ , the wake parameter corresponds to the no-SC TMCI threshold,  $w = 15$ .

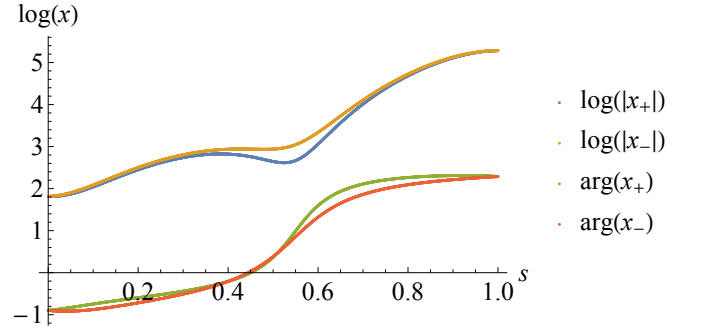


FIG. 16. ACI driven by damping (*sic!*), with the gain  $g = -0.024 = -0.15/T_s$ , for the wake parameter  $w = 7$  and SC parameter  $q = 20$ . Evolution of the initial constant offset  $x^\pm = 1$  is shown after 10 synchrotron periods. Pure convective instability, SCI, for these wake and SC parameters is shown in Fig. 14.

SCI, and at a slightly higher gain the damper triggers the absolute-convective instability. Qualitatively this sequence of stages is the same for all gain phases, although the ACI threshold shows some quantitative dependence on this phase. The reason for this detrimental effect of any center-of-mass damper can be seen in the properties of the non-negative modes at strong SC, presented in Fig. 5. Due to the cobra shapes of the modes, the damper sees only their tails, acting back on the whole bunch proportionally to the tail offset. However, the tail motion is in fact driven by the head, which phase differs by  $l\pi$  from the tail one, where  $l$  is the mode number. Thus, whatever the gain phase, either even or odd modes will get a positive feedback. As a result, for conventional resistive damper, an odd positive mode with the largest coupling with the wake will be most ACI-unstable. For the broadband wake example, presented in Fig. 5, it is the mode  $l = 1$ . Indeed, this very mode can be recognized in the ACI evolution presented in Fig. 16, where

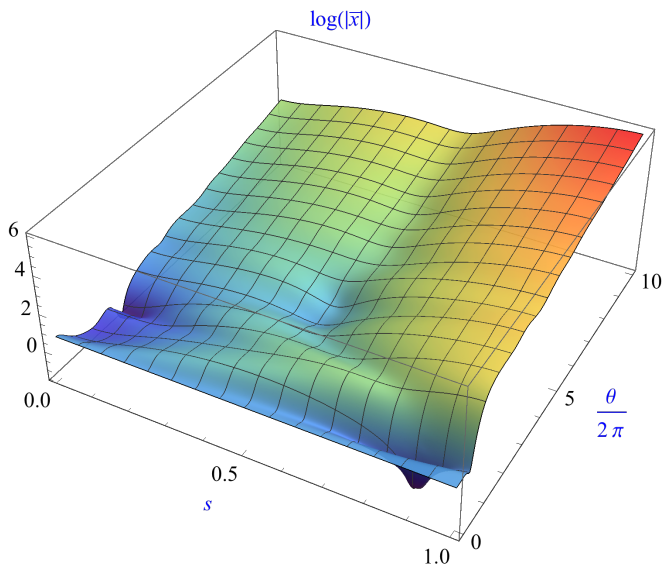


FIG. 17. Time evolution of the ACI for the same parameters as Fig. 16. An exponential growth is clearly seen.

the head-tail phase difference is about  $\pi$ .

#### IV. SUMMARY

Although TMCI wake threshold almost always increases linearly with the SC tune shift,  $w_{th} \simeq w_{th}^0 q/2$ , it does not mean that the beam will be dramatically stabilized by a strong SC. Moving up the TMCI threshold, SC drives the *saturating convective* instability, SCI, and possibly the *absolute-convective* one, ACI, pretty much for the same wake parameters, if not even lower. As a result, the observed intensity threshold can hardly be much larger than its no-SC value; nay, it can be even smaller than that, depending on the injection errors, aperture limitations and coupled-bunch, over-revolution wakes or the presence of a damper: for ACI, even a conventional bunch-by-bunch resistive damper works as its generator. This may explain independence of transverse instability threshold of SC at CERN SPS ring under the old Q26 optics [8–10], with its very large SC parameter,  $2q = \max \Delta Q_{sc}/Q_s = 45$ . The discussed features of the convective instabilities are also compatible with typical absence of nodes at the observed signals of bright proton beams near transition, since the nodes of the initially excited convectively unstable modes overlap with antinodes of their neighbors.

#### ACKNOWLEDGMENTS

I am grateful to Elias Metral and Tim Zolkin for numerous extremely useful discussions.

Fermilab is operated by Fermi Research Alliance, LLC under Contract No. DE-AC02-07CH11359 with the United States Department of Energy.

- 
- [1] A. W. Chao, *Physics of collective beam instabilities in high energy accelerators* (Wiley, 1993).
  - [2] A. Burov, Physical Review Special Topics-Accelerators and Beams **12**, 044202 (2009).
  - [3] V. Balbekov, Phys. Rev. Accel. Beams **20**, 034401 (2017).
  - [4] V. Balbekov, Phys. Rev. Accel. Beams **20**, 114401 (2017).
  - [5] T. Zolkin, A. Burov, and B. Pandey, (2017), arXiv:1711.11110 [physics.acc-ph].
  - [6] R. D. Ruth and J. M. Wang, *APPLICATION OF ACCELERATORS IN RESEARCH AND INDUSTRY. PROCEEDINGS, 6TH CONFERENCE, DENTON, TEXAS, USA, NOVEMBER 3-5, 1980*, IEEE Trans. Nucl. Sci. **28**, 2405 (1981).
  - [7] A. Burov and T. Zolkin, (2018), arXiv:1806.07521 [physics.acc-ph].
  - [8] B. Salvant, *Impedance model of the CERN SPS and aspects of LHC single-bunch stability*, Ph.D. thesis, CERN (2010).
  - [9] D. Quatraro and G. Rumolo, *Proceedings, 1st International Particle Accelerator Conference (IPAC'10): Kyoto, Japan, May 23-28, 2010*, Tech. Rep. (2010).
  - [10] H. Bartosik, *Beam dynamics and optics studies for the LHC injectors upgrade*, Ph.D. thesis, TU Vienna (2013-10-23).
  - [11] E. Metral, *Space Charge 2017 Workshop, Darmstadt, Germany*, (2017).
  - [12] L. Landau and E. Lifshitz, *Fluid Mechanics* (Pergamon Press, 1959).
  - [13] M. Blaskiewicz, Physical Review Special Topics-Accelerators and Beams **1**, 044201 (1998).
  - [14] A. Oeftiger, private communication (2018).